Supporting Information:

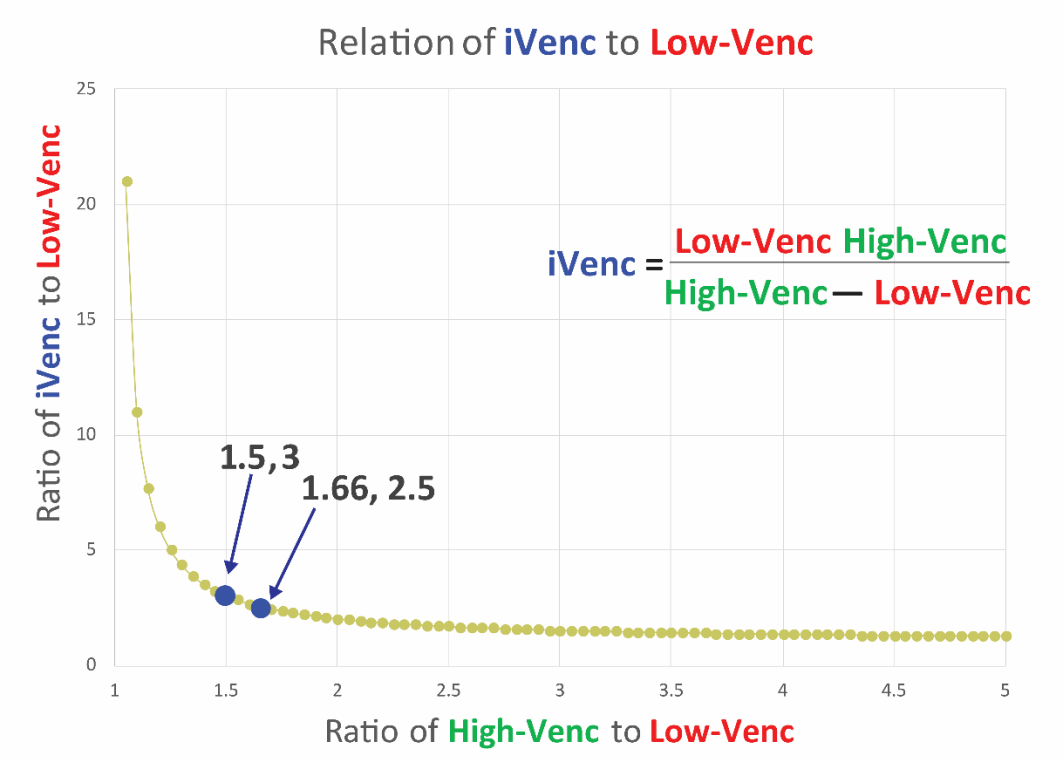

Supporting Information Figure S1: Relationship of the Vencs in triple-Venc encoding. As the high-Venc to low-Venc ratio increases, the iVenc approaches the low-Venc. As the Vencs get closer together, iVenc approaches infinity. The blue dots indicate ratios used in this study.

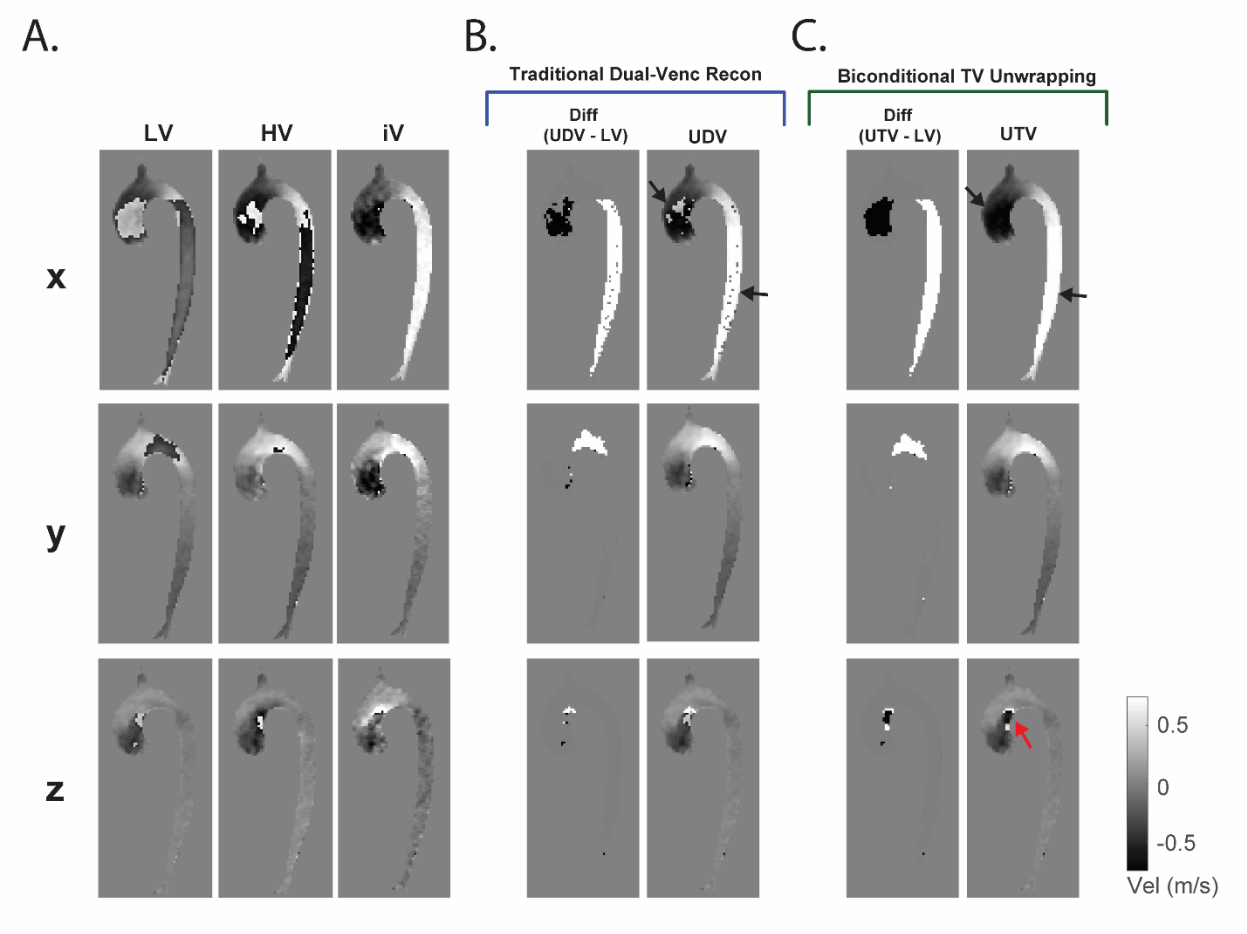

Supporting Information Figure S2: Evaluation of dual-Venc and triple-Venc unwrapping algorithms. I, 50/75/150 representative phase-difference images. All phase-difference images are shown for the same slice location and time point. Both low-Venc (LV) and high-Venc (HV) data show significant velocity aliasing throughout the phantom. The unwrapped dual-Venc (UDV) dataset (B) shows more residual aliasing than the unwrapped triple-Venc (UTV) dataset, which shows successful unwrapping of most voxels, but some residual ones near the vessel wall (red arrows).

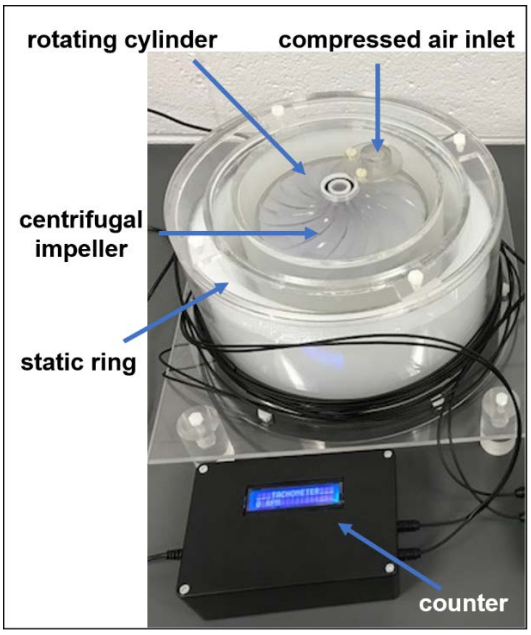

Supporting Information Figure S3: Rotation phantom consisting of a rotating cylinder and a static ring. Compressed air from an external source and the centrifugal impeller drive the rotation of the inner cylinder. A static ring of Gd-doped gel is used for background phase correction. An optical counter with a display screen provides real-time updates on the rotational speed in rotations per minute.

$\mathrm{low-Venc} = \frac{\Pi}{\gamma(\Delta \mathrm{M}_1^{\mathrm{low-Venc}})}$, where

$\Delta \mathrm{M}_1^{(\mathrm{low-Venc})} = \frac{\Delta \mathrm{M}_1^{(\mathrm{low-Venc})}}{2} - \Delta \mathrm{M}_1^{(\mathrm{TR1})}$,

and $\Delta \mathrm{M}_1^{(\mathrm{TR1})} = \Delta \mathrm{M}_1^{(\mathrm{ref})} = -\frac{\Delta \mathrm{M}_1^{(\mathrm{low-Venc})}}{2}$

$\mathrm{high-Venc} = \frac{\Pi}{\gamma(\Delta \mathrm{M}_1^{\mathrm{high-Venc}})} = \frac{\Pi}{\gamma(\mathrm{M}_1^{\mathrm{high-Venc}} - \mathrm{M}_1^{\mathrm{ref}})}$ [2],

Since the high-Venc is inversely proportional to the required gradient moment, with high-Venc>2*low-Venc, where $\Delta M_1^{\mathrm{high}-Venc} < \frac{\Delta M_1^{(low-Venc)}}{2}$in maintaining the same low-Venc gradients as for a conventional 4-point acquisition, the sign of $M_1^{\mathrm{high}-Venc}$, i.e. gradient polarity, needs to be flipped such that $M_1^{\mathrm{high}-Venc} + \frac{\Delta M_1^{(low-Venc)}}{2} < \frac{\Delta M_1^{(low-Venc)}}{2}$. This results in TRs 5-7 (high-Venc) having the opposite first moment polarity of 2-4 (low-Venc).

Supporting Information Figure S4: Brief explanation of gradient polarity flipping for high-Venc > 2*low-Venc. Refer to Figure 1 in the main manuscript for corresponding pulse sequence diagram.

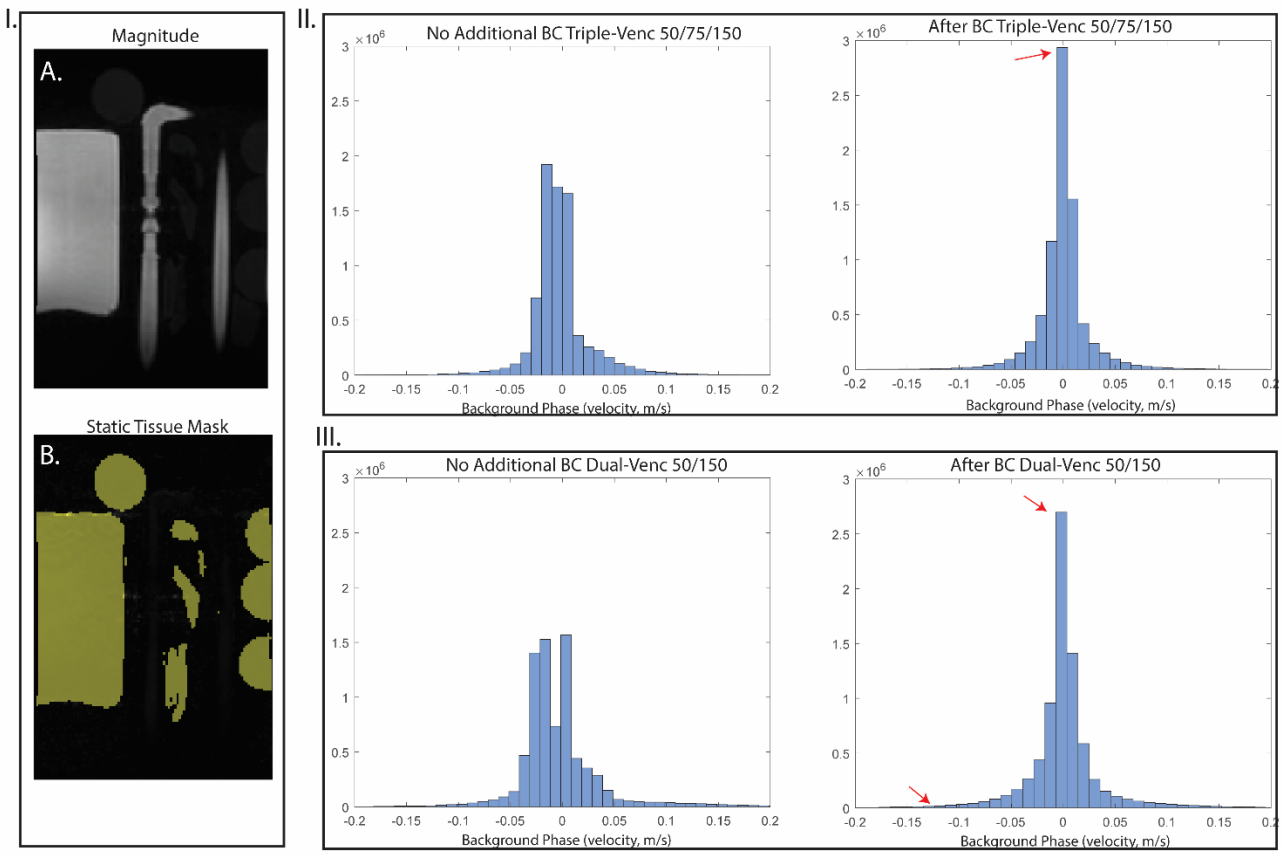

Supporting Information Figure S5: Pulsatile flow phantom background phase/eddy-current effects. I, magnitude image of a central slice in the pulsatile phantom (A) with corresponding manually segmented static tissue mask (yellow, B). II, Histograms of pulsatile phantom background phase quantified over a manually segmented static tissue mask. II and III depict histograms without additional offline second-order background phase correction (BC, left) and the right histograms represent the velocity distribution in the static tissue after background phase correction. Note that after background phase correction[1] more velocities are corrected towards static 0 m/s velocity, however, the dual-Venc acquisition histogram is wider with less velocities in the most central bins (red arrows). Note, correction for Maxwell terms was performed on the scanner.[2]

1. Walker PG, Cranney GB, Scheidegger MB, Waseleski G, Pohost GM, Yoganathan AP. Semiautomated method for noise reduction and background phase error correction in MR phase velocity data. *Journal of Magnetic Resonance Imaging.* 1993;3(3):521-530.
2. Bernstein MA, Zhou XJ, Polzin JA, et al. Concomitant gradient terms in phase contrast MR: analysis and correction. *Magnetic resonance in medicine.* 1998;39(2):300-308.